Research Square

Preprints are preliminary reports that have not undergone peer review.
They should not be considered conclusive, used to inform clinical practice,
or referenced by the media as validated information.

Microbial Signatures in Ancient Desert Environments: Recurrent MISS development from the Mesoproterozoic Mangabeira Formation, Brazil

Amanda de Souza Carvalho Feitosa
amandascfeitosa@gmail.com
Universidade Federal de Santa Catarina
Manoela Bettarel Bállico
Universidade Federal de Santa Catarina
Ezequiel Galvão de Souza
Universidade Federal do Pampa
Claiton Marlon dos Santos Scherer
Federal University of Rio Grande do Sul
Flavia Callefo
University of São Paulo
Vanessa Balbinot
Universidade Federal de Santa Catarina
Gustavo Kube Tatsch
Universidade Federal de Santa Catarina
Adriano Domingos dos Reis
University of Brasília
Elder Yokoyama
University of Brasília
Amanda Moreira Leite
University of Brasília
Sebastião Willian da Silva
University of Brasília
Alexandre Silva Santos
University of Brasília
Alysson Martins de Almeida Silva
University of Brasília
Rodrigo Nunes de Souza
University of Brasília

Article

Keywords: Microbially induced sedimentary structures (MISS), Wet aeolian systems, Proterozoic deserts

Posted Date: May 20th, 2026

DOI: https://doi.org/10.21203/rs.3.rs-9707545/v1

License: This work is licensed under a Creative Commons Attribution 4.0 International License.
Read Full License

Additional Declarations: No competing interests reported.

Microbial Signatures in Ancient Desert Environments: Recurrent MISS development from the Mesoproterozoic Mangabeira Formation, Brazil

Amanda de Souza Carvalho Feitosa[1,+*], Manoela Bettarel Bállico[1,+], Ezequiel Galvão de Souza[2,+], Claiton Marlon dos Santos Scherer[3], Flavia Callefo[4],Vanessa Balbinot[1], Gustavo Kube Tatsch[1], Adriano Domingos dos Reis[5], Elder Yokoyama[6], Amanda Moreira Leite[6], Sebastião Willian da Silva[7], Alexandre Silva Santos[7], Alysson Martins de Almeida Silva[8], Rodrigo Nunes de Souza[8]

[1]Reservoir Geology Laboratory, Department of Geology, Federal University of Santa Catarina, Florianópolis, 88040-900, Brazil.
[2]Geological Modeling Laboratory, Department of Geosciences, Federal University of Pampa, Caçapava do Sul, 97546-550, Brazil.
[3]Institute of Geosciences, Federal University of Rio Grande do Sul, Porto Alegre, 91501-970, Brazil.
[4]Institute of Geosciences, Department of Sedimentary and Environmental Geology, University of São Paulo, 05508-080, São Paulo, Brazil
[5]Graduate Program in Geology, Institute of Geosciences, University of Brasília, Brasília, 70910-900, Brazil.
[6]Laboratory of Magnetic Studies in Geosciences, Department of Geosciences, University of Brasília, Brasília, 70910-900, Brazil.
[7]Optical Spectroscopy Laboratory, Institute of Physics, University of Brasília, Brasília, Federal District, Brazil
[8]Laboratory of Ceramic and Nanostructured Materials, Department of Mechanical Engineering, Faculty of Technology, University of Brasília, Brasília, 70910-900, Brazil.
[*]amandascfeitosa@gmail.com
[+]these authors contributed equally to this work

ABSTRACT

Microbially Induced Sedimentary Structures (MISS) provide some of the most direct evidence of early life–sediment interactions, yet their occurrence in continental eolian systems remains rare. The Mesoproterozoic Mangabeira Formation (São Francisco Craton, Brazil) preserves exceptionally well-developed MISS within an erg-margin succession composed of dunes, interdunes, and dry- and wet eolian sandsheets. Through an integrated stratigraphic, sedimentological, petrographic, and microtextural approach (optical microscopy, Raman spectroscopy, CLSM, and μ-CT), this study reconstructs the environmental and hydrological controls that enabled microbial colonization in an arid continental desert ~1.5 Ga. The vertical succession records six drying-upward cycles governed by fluctuating water-table levels, which periodically stabilized the substrate and promoted microbial mat development. MISS occurs in millimetric laminites characterized by wavy–crinkly lamination, wrinkle textures, mat curling, deformational structures, trapped grains, and organic carbon signatures. Microtextural analyses confirm the presence of kerogen, microbial fabrics, and distinct mineral–organic associations, supporting a biogenic origin. The results demonstrate that microbial communities colonized intermittently wet surfaces during phases of elevated groundwater, stabilizing sediment, trapping fine particles, and generating distinctive biosedimentary textures. These findings highlight the capacity of early microbial ecosystems to occupy extreme terrestrial niches and provide a robust framework for interpreting MISS in ancient continental settings and analogous extraterrestrial environments.

Keywords: Microbially induced sedimentary structures (MISS), Wet aeolian systems, Proterozoic deserts

Introduction

Microbially Induced Sedimentary Structures (MISS) are among the most direct and enduring records of early life-sediment interactions on Earth. Since the establishment of aerobic photosynthesizers, they are formed especially by microbial mats that trap, bind, and stabilize sediments. MISS preserves unique evidence of ecological, sedimentological, and geochemical processes in early environments [1-3]. While well documented in shallow marine settings and tidal environments [4-6], their occurrence in continental deposits is rare[7], offering a unique window into how microbial communities adapted to arid and dynamic terrestrial landscapes. Notably, MISS have also been recorded in proterozoic continental eolian and interdunes deposits [8-10] demonstrating that under certain physicochemical conditions, microbial communities could colonize and leave biosignatures, intermittently wet arid landscapes.

Although the development of microbial mats is commonly associated with shallow aquatic environments, particularly those

linked to the early rise of atmospheric oxygen [11], the presence of MISS in arid continental settings implies that microbial life could also establish itself in extreme terrestrial niches. The colonization of land by microbial life represents a major evolutionary threshold. The first documented morphologically complex Precambrian microfossils, indicated that microbial ecosystems were already widespread and ecologically significant well before the Late Paleozoic [12]. These early communities likely played a central role in shaping Earth's surface environments, particularly through the development of microbial mats capable of interacting with sediments and even producing minerals.

However, microbial colonization of land was not solely a biological process, it was also constrained by geologic and sedimentary conditions. During much of the Precambrian, high siliciclastic sedimentation rates and tectonic instability limited the lateral expansion and preservation of microbial mats. Only after the stabilization of continental basins, through tectonic quiescence and erosional leveling in the late Archaean, did terrestrial environments become suitable for microbial colonization [13]. This shift created more stable sedimentary surfaces that could support mat growth, sediment binding, and the preservation of microbially induced structures.

The Mangabeira Formation of northeastern Brazil [14,15] provides a rare and exceptionally well-preserved record of MISS within an ancient eolian system [16-17]. This formation hosts a variety of microbial features, including biofilm laminations, roll-up structures, and wrinkle textures. The sedimentary succession records the accumulation of a desert paleoenvironment characterized by eolian dunes, wet and dry sandsheets, and wadi deposits organized into drying-upward cycles [18,19]. The outcrops analyzed in this study are located in the central area of the Chapada Diamantina Domain (Fig. 1), within São Francisco Craton, northeastern Brazil, where both microbial and non-microbial sedimentary structures are exceptionally preserved (Fig. 1). Radiometric dating constrains the formation to approximately 1.5 Ga, based on swarms of tholeiitic mafic dikes and sills intruding its basal portion, with a maximum depositional age of 1.6 Ga [20,21].

In this study, we employ a multi-proxy approach, integrating stratigraphy, sedimentary architecture, petrography, and geochemical analyses. This combination allows us to reconstruct environmental conditions, sedimentary dynamics, and microbial adaptations that governed MISS formation in arid continental settings. While the detailed implications for microbial evolution, atmospheric oxygenation, and Precambrian paleoecology are explored further in our discussion, the Mangabeira record provides a compelling glimpse into how microbial communities colonized and persisted in one of Earth’s earliest desert environments.

By highlighting the interplay between microbial innovation, sedimentary processes, and paleoenvironmental conditions, this study underscores the importance of MISS as both agents and recorders of early terrestrial ecosystems. These findings not only advance our understanding of early life on land but also establish a framework for interpreting MISS in other ancient continental settings—and potentially in extraterrestrial environments where analogous sedimentary features may preserve traces of past microbial activity.

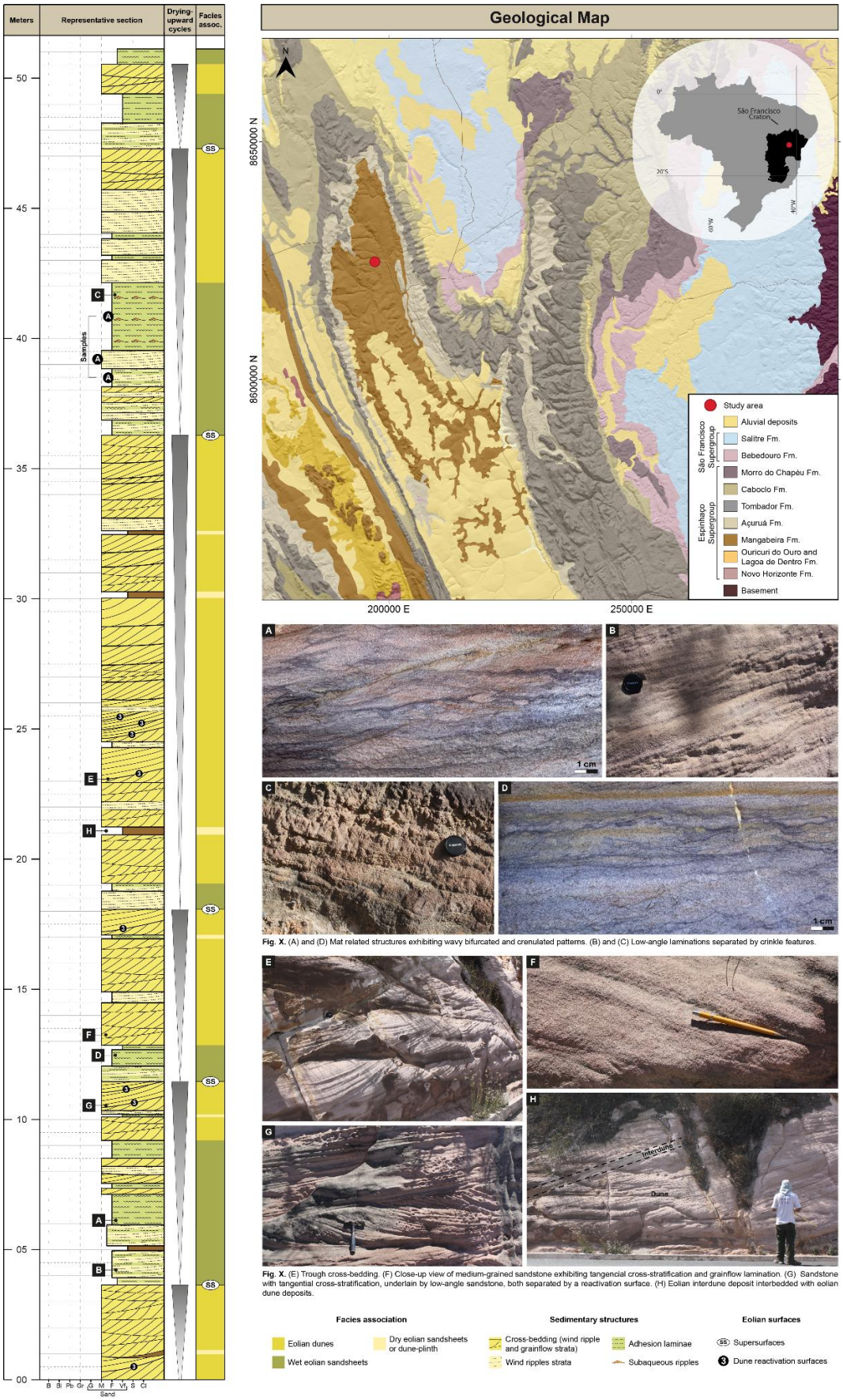


Fig. X. (A) and (D) Mat related structures exhibiting wavy bifurcated and crenulated patterns. (B) and (C) Low-angle laminations separated by crinkle features.

Fig. X. (E) Trough cross-bedding. (F) Close-up view of medium-grained sandstone exhibiting tangencial cross-stratification and grainflow lamination. (G) Sandstone with tangential cross-stratification, underlain by low-angle sandstone, both separated by a reactivation surface. (H) Eolian interdune deposit interbedded with eolian dune deposits.

Figure 1: Synthesis of the main elements analyzed in this study, including the detailed stratigraphic column of the succession, the geological map of the study area, and representative images of the sedimentary features and structures observed in the field.

Results

Depositional Context

Throughout the studied ~51 m-thick vertical succession, a well-defined cyclic sedimentation pattern was recognized. Six cycles were identified, each displaying a consistent vertical facies arrangement (Fig. 1). The cycles range from 3 to 18 m in thickness and are bounded at their base and top by laterally extensive, nearly horizontal surfaces. The basal portions of each cycle consist of very fine- to medium-grained, moderately sorted sandstones organized into low-angle (<5°) tabular layers, 1.0–10 m thick and laterally traceable for up to 20 m. Internal structures occur as 0.8–2.6 m thick packages that include: (i) inverse-graded, horizontally to low-angle translatent lamination (sets 0.2–0.8 m thick); (ii) tangential cross-stratified sandstones in lenticular, discontinuous sets up to 0.2 m thick, with grain flow and wind-ripple lamination; and (iii) interlayered sandstone–mudstone with crinkly lamination (sets 0.2–2.6 m thick, traceable for up to 20 m). Upsection these deposits are vertically succeeded by fine- to medium-grained sandstones, well- to subrounded and well- to bimodally sorted, arranged in tabular sandstone bodies, 1.2-17.2 m thick, laterally continuous up to 20 m, display wedge- and trough-shaped sets bounded by planar to gently inclined surfaces (<5°). Internally, these sandstones are composed of alternating grain-flow laminae and wind-ripple lamination.The deposits are organized into small-scale sets of eolian cross-strata (up to 0.2 m thick) that gradually increase in thickness upward, culminating in medium- to large-scale eolian cross-strata dunes (up to 1.2 m thick) (Fig. 2).

Interpretation:

The tabular package compounded by inverse-graded, horizontally to low-angle translatent lamination are interpreted as are related to subcritical climbing translatent strata formed in an aeolian sand sheets context [22,23,18]. The cross-strata sets that occur intercalated suggests isolated aeolian dunes separated by extensive areas of aeolian sand sheets [24,25,18]. The sandstone–mudstone with crinkly lamination are interpreted as high frequency intercalation of subaqueous, aeolian and microbial deposits whose origins will be detailed below. The large-scale cross-bedding, comprising grainflow and wind-ripple laminae are interpreted as residual deposits of eolian dunes, bounded by interdune surfaces ascribed to the successive climbing of eolian dunes [18]. The vertical stacking of facies defines a consistent drying-upward trend, which is systematically repeated through the succession (Fig. 2). Each cycle begins with water-lain and eolian sandsheet deposits that grade upward into eolian dune and facies. The progressive drying-upward trends, capped by laterally extensive bounding surfaces, reflect changing wet to dry eolian conditions within an eolian system [18]. Each cycle represents successive phases of dune-field accumulation, stabilization, and deflation, controlled by variations in sediment supply, wind regime, and water-table position [26]. The basal wet eolian sandsheets and waterlain deposits represent intervals of high water-table conditions, where microbial mats developed under reduced sand mobility. Internally, the repetitive small-scale cycles are formed in conditions where progressive drying increased the availability of loose sand, promoting the accumulation of wind ripples strata and the formation of small-scale dune sets. The upper portions of each drying-upward cycle are dominated by medium to large-eolian dune deposits formed under low water-table conditions, allowing sand mobilization by wind [26]. Accumulation within these dry eolian systems occurred when a positive sediment budget was achieved, driven by sufficient sand supply, reduced transport rates, and dune migration that promoted progressive stacking and surface coverage by aeolian bedforms. Each cycle is bounded by laterally extensive deflationary supersurfaces that truncate underlying dune strata, marking phases of non-deposition and erosion related to negative sediment budgets [18]. The repetition of these cycles, capped by planar supersurfaces, records recurrent episodes of dune-field construction, stabilization, and deflation under fluctuating climatic and hydrological conditions [18].

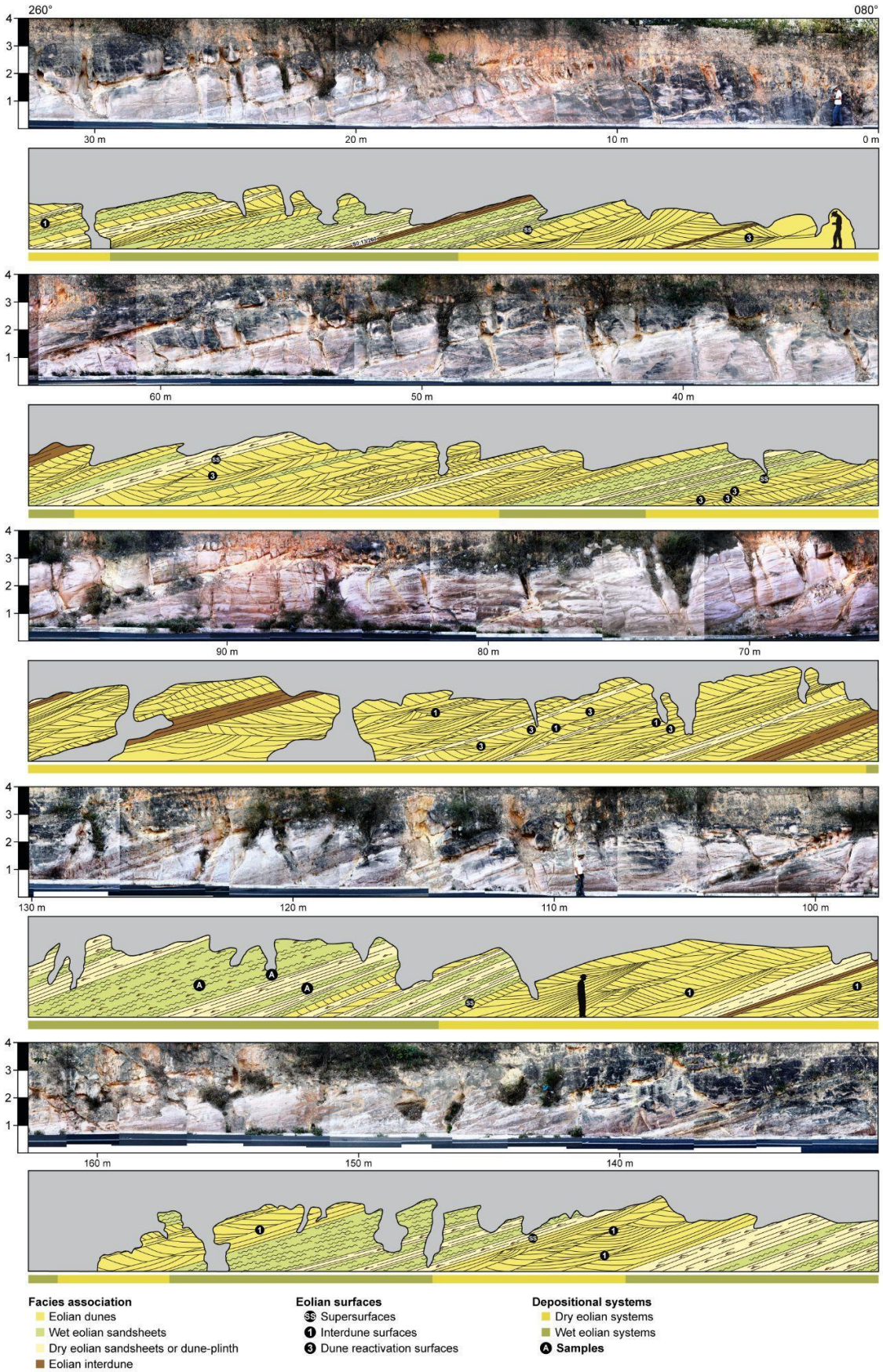


Figure 2: Interpreted photomosaic showing the organization of facies within the eolian succession. The transition from water-lain/eolian sandsheets to cross-bedded dune deposits reflects a consistent drying-upward pattern, with bounding surfaces marking the top of each cycle and recording periods of dune stagnation or interdune flooding.

Microbial mat-related macro- and microstructures

The Mangabeira Formation represents an extensive aeolian succession comprising dune, interdune and wet sandsheet deposits that developed under fluctuating groundwater levels within a semi-arid setting [18, 19]. Within these deposits, microbial activity produced distinct sedimentary structures, ranging from macroscopic features observable in outcrops to microscopic textures revealed through petrographic analysis. These microbial structures are particularly well developed within wet eolian sandsheets deposits, where periodic fluctuations in moisture conditions favored the stabilization of sediment surfaces and the preservation of microbial mats.

Microbial mat fabric

At the macroscopic scale, the MISS-bearing intervals are composed of lighter and darker laminations, millimetrically spaced and laterally continuous with ~20 cm width (Fig. 3).The lighter laminations are composed of very fine- to fine-grained sandstones, moderately sorted, with angular to subangular grains, and are structureless. In cross-sections, these sandy portions are commonly laterally continuous, although in some cases they are discontinuous and occasionally develop concentric fragment-like features (Fig. 3C-D). The dark laminations are arranged in millimetric- to centimetric-thick, sub-horizontal or diffuse laminae, with irregular laminations and predominantly diffuse contacts with the sandy portions. The drapes show considerable variation in thickness, and their morphology is characterized by crenulated to wavy (wrinkle) lamination, with undulation amplitudes reaching up to 0.5 cm. The crinkly laminations display micro-rugosities, discontinuous crests, and even small ripples, although the latter are restricted to portions with reduced microbial biofilms. Laterally, they exhibit a pattern of bifurcation and lateral coalescence, in which the laminae split into multiple branches that later merge with adjacent laminae. In thin sections, these millimetric facies exhibit additional characteristics (Fig. 3).

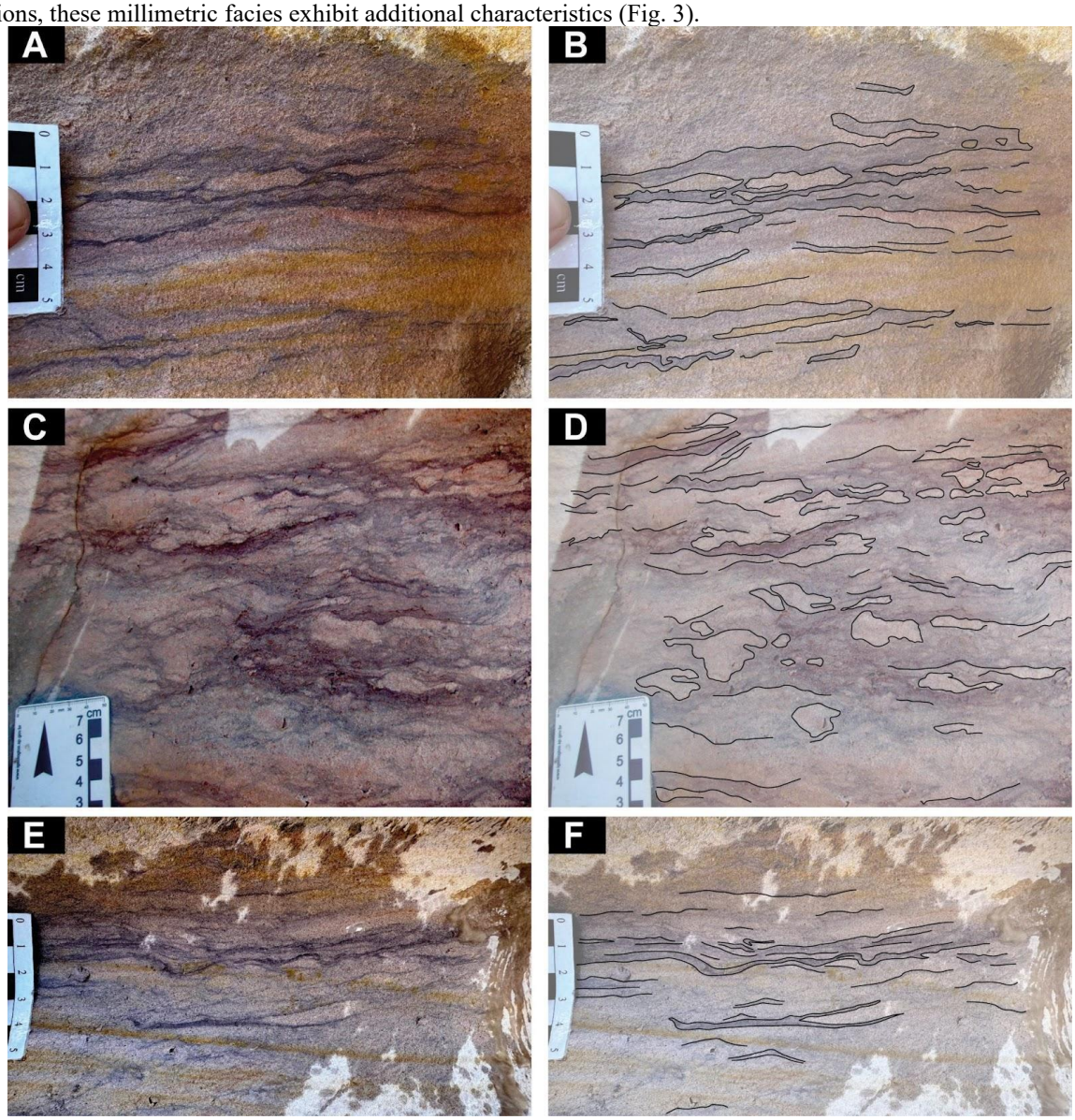


Figure 3: Different morphologies of mud drapes were identified, including disoriented forms, mixtures with coarse sand, concave and wavy geometries, dispersive tails, bifurcated and crenulated patterns, sub-horizontal layering, and rough or diffuse textures. Images are shown on the left and the corresponding interpretations on the right.

The sandy intervals (Fig. 4) are sparsely colonized by biofilms and encompass grain sizes ranging from 53 μm to 2603 μm, being composed predominantly of angular quartz and feldspar grains, with the local occurrence of millimetric lithic fragments, in which poor grain-size sorting predominates. In contrast, the finer-grained and better-sorted deposits (dark laminations) (Fig. 4) show a greater abundance and improved preservation of microbial structures.

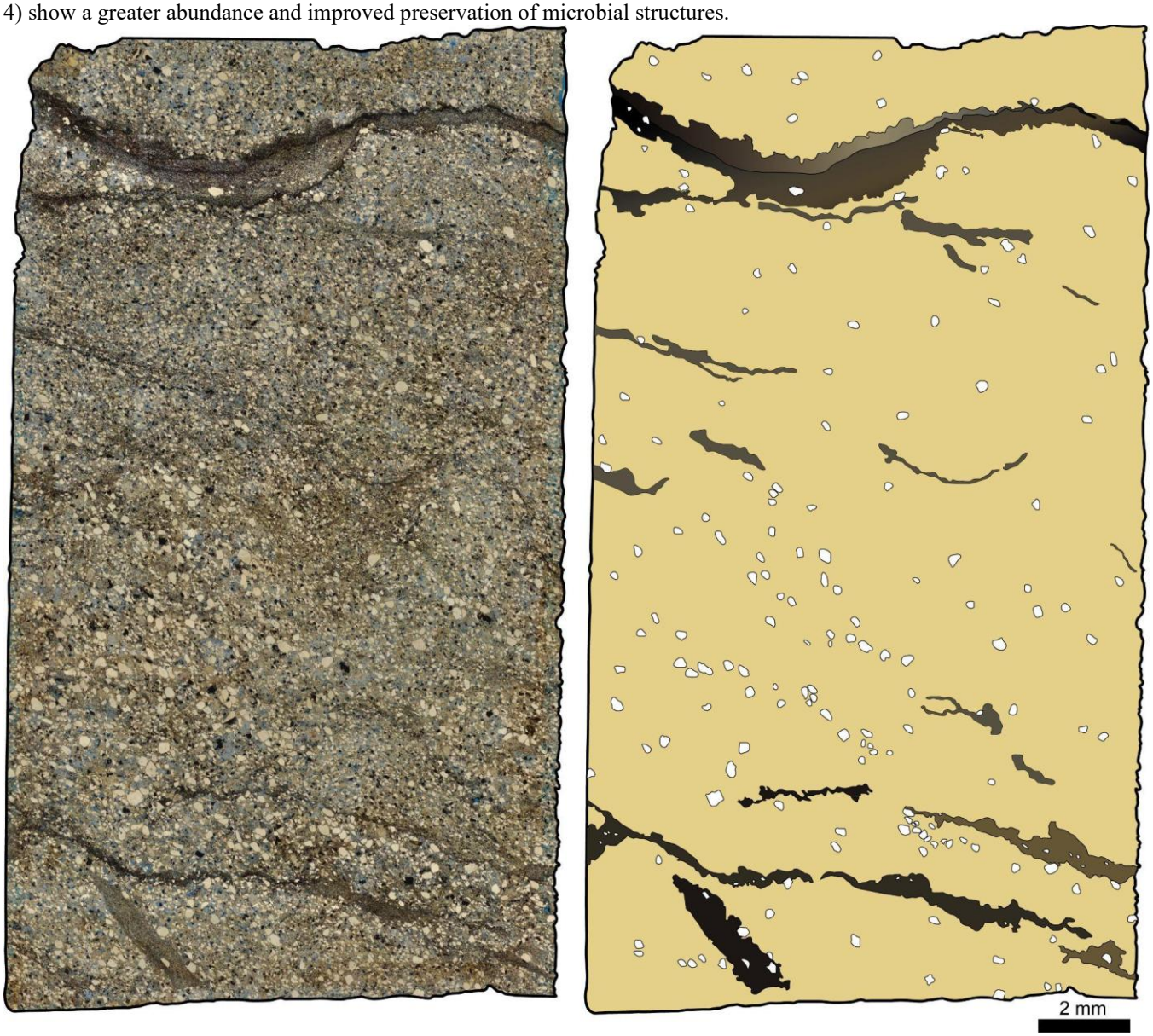


Figure 4: Mosaic highlighting alternations between light and dark laminae. The dark laminae appear more discontinuous at the bottom and more continuous at the top.

The finer intervals range from 8.9 μm to 761 μm and are composed of silty to very fine sandy laminae. The microbial mats exhibit greater lateral continuity, better grain-size sorting, and a lower incidence of physical disturbances. Within these horizons, several microbial structures occur, such as shallow depressions related to mat–sediment interaction; wavy-crinkly lamination (Fig. 5A-B), displaying undulated to crinkled laminae distinct from the parallel laminations typical of settling; authigenic mineral associations enriched in pyrite, often linked to convolute features (Fig. 5C-D); curled-up mats, exhibiting folds and rotations of up to 180°, forming structures up to 17 mm thick (Fig. 5E-F); and mat fragments with frayed edges (Fig. S8 E-F), discontinuous and associated with deformed laminae and disoriented mica grains (Fig. S8 C-D) up to 0.6 mm trapped within microbial filaments, showing variable orientations with preferential alignments in the NE–SW and E–W quadrants.
These structures result from the interaction between microbial mat growth and low-energy hydrodynamic processes, in which cohesive biofilms induce small-scale plastic deformation and the trapping of fine particles. Consequently, the MISS-bearing intervals, with light and dark laminations, record penecontemporaneous biostabilization of sediment and limited sediment movement, reflecting distinct stages of microbial mat development and stabilization [27, 28]

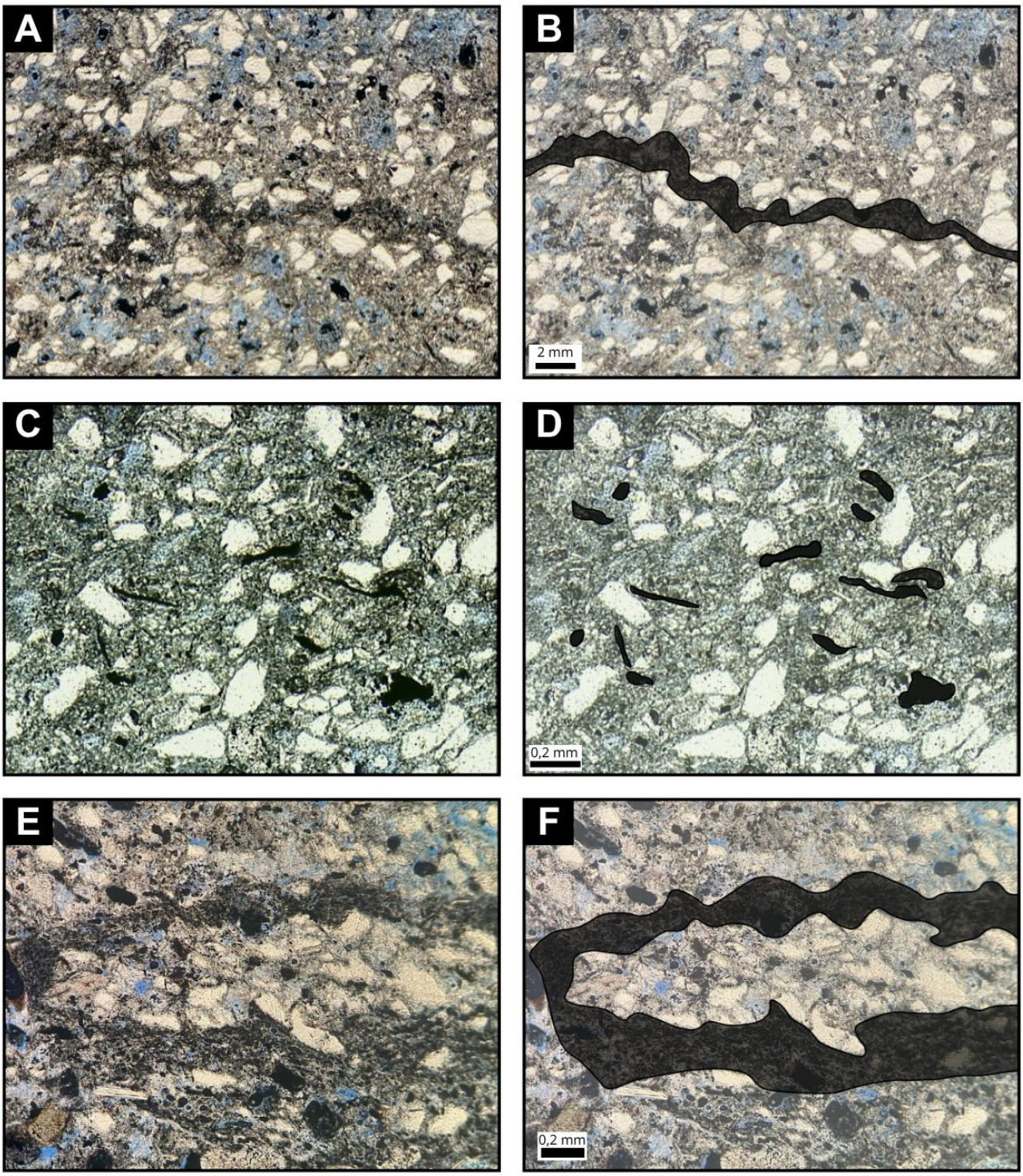


Figure 5: Identified MISS under optical microscopy: (A) Predominance of wavy–crinkly structures; (B) Sketch highlighting the MISS; (C) Associations of authigenic minerals with pyrite enrichment; (D) Sketch highlighting the MISS; (E) Rolled-up mat structures; (F) Sketch highlighting the MISS.

Microtextural analyses

Raman Spectroscopy

The Raman spectrum, presented in Fig. 6, reveals a biogenic organic matrix composed of thermally immature carbonaceous material, whose characteristics are consistent with Type I or Type II kerogen. The predominance of the D1 (1360 cm^{-1}) and D3 (470 cm^{-1}) bands relative to the G band (1585 cm^{-1}), together with the presence of the D2 band (1610 cm^{-1}), is diagnostic of kerogen enriched in amorphous carbon and molecular-scale defects. Moreover, the coexistence of the TiO_2 (rutile) phase, characterized by peaks at 448 and 611 cm^{-1}, and iron oxide (hematite), with bands at 226, 294, and 415 cm^{-1}, suggests that the mineralization process was mediated by microbial biomass. In this scenario, the sequestration of metallic cations by microbial

exopolymers likely preceded partial phase transitions, thereby preserving a distinctive geochemical record of the thermal and redox evolution of the sedimentary paleoenvironment.

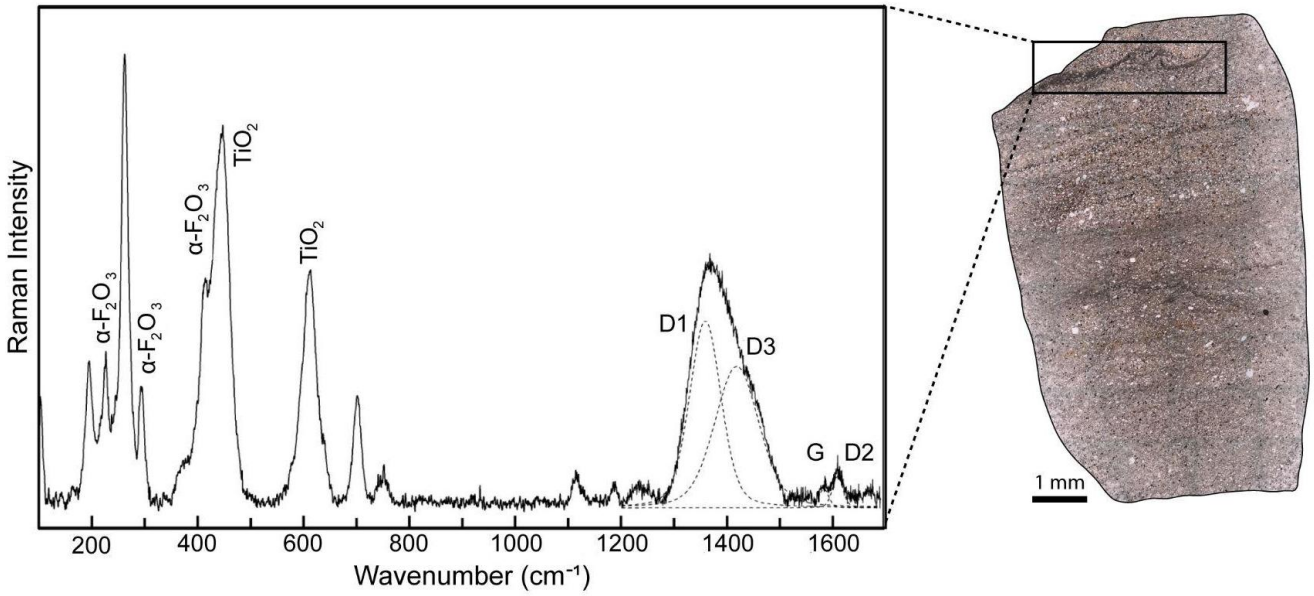


Figure 6: Raman spectrum of MISS sample. The dashed lines represent deconvolutions of the overlapping bands D1, D2, D3 and G.

Confocal fluorescence microscopy

Strong fluorescence was detected in both the red and green channels, indicating the presence of organic compounds capable of excitation and emission within these spectral ranges. In geological samples, such fluorescence commonly reflects the presence of aromatic carbon structures, kerogen, and remnants of extracellular polymeric substances (EPS) preserved within microbial textures. Red-channel emission is typically associated with more thermally mature or aromatic organic compounds, while green fluorescence may reflect less mature organic residues or mineral-bound organic films. Together, these signals support the interpretation that the sample retains preserved organic material consistent with microbial activity. Visual representatives can be observed in the supplementary data.

Micro-computed tomography

Quantitative analysis revealed that 21.2% of the volume (6.47×10^{12} µm³) corresponds to material associated with bacterial activity, 52.3% (2.62×10^{12} µm³) to the rock matrix, and 26.5% to pore volume. Higher X-ray intensity was observed in microbially active portions, reflecting the greater density of this phase. Areas with higher Fe_2O_3 density were identified and interpreted as resulting from bacterial activity, forming the microbial mats. The morphology of these portions displayed well-defined undulations and wrinkles, consistent with features previously recognized in the facies analysis of the sedimentary unit. Additionally, curled features up to 2 mm wide were observed, supporting the interpretation that these structures result from the interaction between depositional dynamics and surface stabilization by microbial communities, associated with desiccation under arid conditions. Visual representatives can be observed in the supplementary data.

Interpretations

The sedimentological framework records an aeolian system modulated primarily by fluctuations in the water table, which controlled substrate moisture and, consequently, the establishment and preservation of microbial communities. The alternation between poorly sorted sandy intervals and fine-grained, laminated horizons reflects shifts between drier conditions with limited microbial activity and wetter phases linked to a higher water table, during which surface stabilization promoted microbial colonization. The silty intervals with well-preserved structures represent periods of reduced reworking and sustained moisture availability, allowing the development of cohesive microbial mats. Within these intervals, wavy-crinkly laminations (Fig. 5A-B) are interpreted as the expression of mat growth and sediment trapping, preserving irregular biogenic surfaces that were later compacted but retained their primary morphology [4]. Features such as convolute structures associated with authigenic mineral enrichments (Fig. 5C-D) and the disoriented distribution of mica grains (Fig. S8 C-D) reflect the interaction between sediment particles and a cohesive extracellular polymeric matrix, in which grains were trapped and prevented from maintaining hydrodynamic orientation [29]. These characteristics indicate that microbial activity, modulated by water table oscillations, governed sediment organization and early diagenetic processes, including the establishment of geochemical gradients and localized mineral precipitation. Episodes of water table lowering led to desiccation and contraction of the biofilm, generating cavities, internal deformation, and the development of curled (Fig. 5E-F) and fragmented mat structures, which record repeated phases of exposure, shrinkage, and cohesion loss under arid to semi-arid conditions. Analytical data further support this interpretation, as Raman spectroscopy indicates the preservation of thermally immature, defect-rich carbonaceous material consistent with low-grade kerogen, while the association with mineral phases such as rutile and hematite suggests microbially

mediated mineralization. Confocal fluorescence microscopy confirms the presence of preserved organic compounds with varying degrees of aromaticity, and micro-computed tomography reveals a significant volumetric contribution of dense, iron-rich, microbially influenced material displaying morphologies consistent with mat structures. Together, these observations indicate that fluctuations in the water table were the primary control on microbial activity, sediment stabilization, and the preservation of biosignatures within the depositional system.

Discussion

Genesis of Mat Structures in the Wet Eolian Sandsheets

During Precambrian time, microbial communities progressively expanded beyond coastal and shallow-marine settings, adapting to increasingly extreme continental conditions such as desiccation, fluctuating salinity, intense ultraviolet radiation, and long-distance wind transport [30]. The development and persistence of these microbial communities depended on specific environmental conditions, including the availability of water, sufficient light, suitable temperatures, low hydrodynamic energy, and prolonged periods of non-burial [4]. Such requirements are consistent with the environmental framework recorded in the Mangabeira Formation, where repeated alternations between wet and dry aeolian conditions created transient ecological windows favorable for microbial colonization.

The earliest occurrences of MISS in fully continental environments, associated with eolian interdune deposits, date to around ~2.0 Ga [8,9]. Wind-driven dispersal, as observed in modern deserts such as the Atacama [31], likely played a fundamental role in enabling cyanobacteria and other microorganisms to colonize vast continental areas, contribute to biogeochemical cycling, and establish early continental ecosystems [31]. Furthermore, microorganisms have developed the ability to protect themselves from high levels of UV radiation through the production of EPS, which can act as a shield for the bacterial community, among other benefits. The EPS protects microorganisms from radiation (especially UV, and in some cases reducing the indirect effects of ionizing radiation) by absorbing/attenuating photons, scattering, retaining antioxidant compounds, and scavenging/neutralizing reactive species [32-35], a mechanism well documented in modern biological soil crusts (BSC) [36]. This milestone indicates that significant changes occurred in microbial composition and physiology, including the production of wax esters [37,38] and the development of oscillatory gliding mechanisms [12], which conferred greater resistance to intense hydration and desiccation cycles. The sedimentological record of the Mangabeira Formation provides direct evidence of similar processes operating along a Proterozoic erg margin, where cycles of aeolian accumulation and deflation were strongly modulated by groundwater table fluctuations.

In this setting, climatically controlled oscillations between wet and dry conditions strongly influenced the large-scale depositional style. During wetter phases, accumulation occurred on moisture-rich substrates, where the capillary fringe periodically intersected the depositional surface, promoting the development of wet eolian systems. During drier phases, deposition took place in fully dry, wind-dominated environments characteristic of dry eolian systems [26]. This cyclic alternation, is also documented in analogous Proterozoic and Phanerozoic eolian systems [39-42, 10, 18], resulted in repetitive drying-upward successions.

The widespread occurrence of microbially induced sedimentary structures (MISS) in the Mangabeira Formation is closely linked to wet eolian system dynamics, as their formation requires sustained intervals of substrate moisture that enable microbial communities to bind and stabilize sediment. Multiple MISS-bearing cycles are preserved, each reflecting a strong coupling between hydrological fluctuations and microbial activity. Consequently, these deposits comprise fine-grained sandstones containing MISS that alternate with dry eolian sandsheet deposits and small dune units. Such cyclicity reflects short-term oscillations in groundwater table elevation and surface moisture availability.

Once established, microbial mats markedly increase substrate resistance to wind action. Even under high wind velocities, mat-covered surfaces exhibit enhanced cohesion that strongly limits sand transport [10]. As a result, sediment availability at the surface decreases, restricting the formation of small eolian bedforms and favoring the accumulation of moist sandsheets. These conditions, in turn, promote further microbial colonization, reinforcing a positive feedback between sediment stabilization and microbial mat development [43, 44, 10]. As a consequence of this stabilization, wind-transported sediments moving across the mat surface can be efficiently trapped, bound, and aggregated [45, 10], resulting in features such as mat-layer-bound fine grains (Fig. 4) and selectively concentrated heavy minerals (Fig. 5C-D). In addition, smooth surface depressions formed through the interaction between the cohesive microbial mat and the underlying unconsolidated sediment. In such cases, substrate deformation is limited by the mechanical strength of the biogenic matrix, producing subtle surface relief features [4].

Subsequent groundwater table lowering promoted surface desiccation, increased sand mobility, and resulted in the accumulation of wind-ripple strata and small dune sets. During these phases, features such as roll-up structures and mat curls developed. These structures form because the upper layer of the microbial mat retains higher moisture content; during desiccation, the ductile behavior of biofilms causes the mat layers to curl upward [4].

During intervals when sedimentation rates were very high, they exceeded the specific thresholds for biostabilization and baffling-and-trapping [46]. Wind reworking locally disturbed microbial surfaces; however, limited eolian activity could coexist with microbial stabilization, allowing the development of small-scale eolian ripples [47]. Such reworking is evidenced by frayed mat edges and deformed microbial features (Fig. S8 E-F).

The dynamic balance between moisture availability, microbial activity, and sediment transport ultimately governs the preservation potential of these MISS. Mat cohesion, sediment trapping, and mucilage production occur preferentially during wet phases, whereas desiccation suppresses microbial motility and enhances surface stabilization. Studies of modern microbial mats [47] emphasize the key role of the capillary fringe in regulating surface moisture. Small shifts in groundwater table

elevation control the duration of mat exposure, the frequency of desiccation events, and the potential for preservation.
Groundwater table fluctuations played a fundamental role in the generation and preservation of MISS within these wet eolian sandsheets. Periods of groundwater rise, when the water table intersected the sediment surface, increased substrate moisture, promoting microbial activity and enabling the development and cohesion of microbial mats. In contrast, phases of groundwater lowering led to drier surface conditions, favoring the accumulation and preservation of dry eolian deposits in the absence of sustained surface moisture. In the Mangabeira Formation, such groundwater-controlled moisture variations produced only subtle surface modifications, sufficient to regulate microbial colonization without inducing significant sediment reworking. This allowed microbial mats to establish, persist, and be preserved through repeated wetting and drying cycles controlled by groundwater oscillations. These delicate signatures indicate that microbial mats were resilient to low-magnitude hydrodynamic variability, primarily governed by autogenic eolian–hydrogeological processes. Taken together, the sedimentological and microbially induced features of the Mangabeira Formation record a dynamic wet–dry regime linked to groundwater table fluctuations along Proterozoic erg margins. This composite record highlights how subtle hydrodynamic variations at centimeter- to meter-scale were superimposed on longer-term climatic controls, producing a sensitive archive of environmental instability in early continental eolian systems.

Conclusions

The record of the Mangabeira Formation unequivocally demonstrates that microbial colonization in Mesoproterozoic arid continental environments was neither episodic nor marginal, but rather a recurrent process controlled by subtle and highly sensitive hydrological fluctuations. The integration of sedimentological, petrographic, and microtextural evidence confirms the biogenic origin of MISS and reveals that variations in groundwater levels played a central role in creating ecological windows that enabled the establishment, growth, and preservation of microbial mats.
These findings show that, even under extreme environmental conditions, microbial communities were capable of stabilizing sediments, modulating depositional processes, and generating complex biosedimentary signatures that could be preserved in the geological record. In this context, the Mangabeira Formation not only expands our understanding of early life adaptation in continental settings, but also redefines the role of wet eolian systems as key archives of biosphere–geosphere interactions on early Earth. Beyond its regional significance, this study establishes a robust framework for the identification and interpretation of MISS in ancient continental settings, providing a valuable tool for paleoenvironmental reconstructions and for the search for biosignatures in analogous extraterrestrial environments.

Methods

These MISS provide valuable insights into the interactions between microbial communities and sedimentary processes, including deposition, biostabilization, and early diagenetic mineralization. To characterize these features, integrated faciological and petrographic analyses were conducted, allowing the identification of key lamination types, mat morphologies, and authigenic mineral assemblages indicative of microbial activity and environmental variability within the eolian system. A combination of analytical techniques was employed, including optical microscopy, Raman spectroscopy, confocal fluorescence microscopy, and micro-computed tomography, to comprehensively characterize the samples.

Raman Spectroscopy

Raman microspectroscopy analysis was performed using LabRAM HR Evolution (HORIBA, Scientific, Palaiseau, France) equipped with an 1800 lines/mm grating and CCD detector. Measurements were conducted with 532 nm laser excitation source (1 mw) focused on the samples by an OLYMPUS microscope with a x50 objective. To obtain the spectra, 10 accumulations of 10 seconds each were used, and subsequently, baseline and normalization were performed on the spectra using the LabSpec and OriginPro programs.

Confocal Fluorescence Microscopy

Confocal Laser Scanning Microscopy (CLSM) was carried out using a Leica TCS SP5 confocal microscope, equipped with multiple excitation sources, including a 405-nm diode laser, 488- and 514-nm argon lasers, and 543-, 594-, and 633-nm HeNe lasers. The system includes a motorized Leica DMI6000 CS stand with a trinocular tube, two 10×/22 BR.M eyepieces, a control unit, and a transmitted-light illumination column. The microscope is fitted with objectives of 5× (dry), 10× (dry), 20× (oil/water), 40× (oil), and 63× (oil), allowing the acquisition of high-resolution optical sections. Imaging was performed in fluorescence mode, enabling the acquisition of z-stacks and subsequent three-dimensional reconstruction based on optical sectioning. This configuration is particularly well-suited for the visualization of microbial biofilms and micro-scale sedimentary structures. Fluorescence image stacks were acquired in xyz mode at 1024 x 1024 pixels. For high-resolution scans, the field of view was approximately 260-300 µm, corresponding to a pixel size of ~0.26-0.29 µm in the xy-plane. The confocal pinhole was set to 120 µm (~2 Airy units). Excitation was provided by the 405-nm diode laser, with the acousto-optical tunable filter (AOTF) set to 48% of the maximum output, and fluorescence was collected on PMT3 with a high voltage of 875 V. The z-step was set to 0.05 µm. Imaging parameters were kept constant across all analyses to ensure reproducibility.

Microcomputed Tomography

Microcomputed Tomography (Micro-CT) was performed using a Thermo Fisher HeliScan Mk. I system, configured with 3-mm steel filters, an X-ray tube voltage of 140 kV, a current of 60 µA, and an exposure time of 0.25 s, operating along a double-

helix scanning trajectory. The resulting voxel size for the analyzed sample was 32.7 μm, providing a resolution suitable for the aims of this study. Low-resolution reconstruction was carried out using the Filtered Back Projection (FBP) algorithm, executed in a high-performance computing environment. The resulting TIFF image stack was then organized, compiled, and processed during the high-resolution reconstruction stage using Avizo (Thermo Scientific), a specialized software for three-dimensional image processing. The experimental setup was defined to ensure reproducibility and to enable quantitative comparison with Scanning Electron Microscopy (SEM) analyses.

References

[1] Noffke, N., Gerdes, G., Klenke, T. & Krumbein, W. E. Microbially induced sedimentary structures - Examples from modem sediments of siliciclastic tidal flats. *Zentralblatt für Geologie und Paläontologie* **1995**, 307-316 (1996).

[2] Gehling, J. G. & Droser, M. L. Textured organic surfaces associated with the Ediacara biota in South Australia. *Earth-Science Reviews* **96**, 196–206, DOI: https://doi.org/10.1016/j.earscirev.2009.03.002 (2009).

[3] Shepard, R. N. & Sumner, D. Y. Undirected motility of filamentous cyanobacteria produces reticulate mats. *Geobiology* **8**, 179-190, DOI: https://doi.org/10.1111/j.1472-4669.2010.00235.x (2010).

[4] Schieber, J., Bose, P. K., Eriksson, P. G., Banerjee, S., Sarkar, S., Altermann, W. & Catuneanu, O. (eds.) *Atlas of microbial mat features preserved within the siliciclastic rock record* (Elsevier, 2007).

[5] Noffke, N., Beukes, N., Gutzmer, J. & Hazen, R. M. Spatial and temporal distribution of microbially induced sedimentary structures: A case study from siliciclastic storm deposits of the 2.9 Ga Witwatersrand Supergroup, South Africa. *Precambrian Research* **146**, 35–44, DOI: https://doi.org/10.1016/j.precamres.2006.01.003 (2006).

[6] Noffke, N., Beukes, N., Bower, D., Hazen, R. M. & Swift, D. J. P. An actualistic perspective into Archean worlds - (cyano-)bacterially induced sedimentary structures in the siliciclastic Nhlazatse Section, 2.9 Ga Pongola Supergroup, South Africa. *Geobiology* **6**, 5–20, DOI: https://doi.org/10.1111/j.1472-4669.2007.00118.x (2008).

[7] Beraldi-Campesi, H., Farmer, J. D. & Garcia-Pichel, F. Modern terrestrial sedimentary biostructures and their fossil analogs in Mesoproterozoic subaerial deposits. *PALAIOS* **29**, 45-54, DOI: http://dx.doi.org/10.2110/palo.2013.084 (2014).

[8] Eriksson, P. G., Simpson, E. L., Eriksson, K. A., Bumby, A. J., Steyn, G. L. & Sarkar, S. Muddy roll-up structures in siliciclastic interdune beds of the c. 1.8 Ga Waterberg Group, South Africa. *PALAIOS* **15**, 177-183, DOI: https://doi.org/10.2307/3515640 (2000).

[9] Simpson, E. L., Heness, E., Bumby, A., Eriksson P. G., Eriksson K. A., Hilbert-Wolf, H. L., Linnevelt, S., Malenda, H. F., Modungwa, T. & Okafor, O. J. Evidence for 2.0 Ga continental microbial mats in a paleodesert setting. *Precambrian Research* **237**, 36-50, DOI: http://dx.doi.org/10.1016/j.precamres.2013.08.001 (2013).

[10] Basilici, G., Soares, M. V. T., Mountney, N. P. & Colombera, L. Microbial influence on the accumulation of Precambrian aeolian deposits (Neoproterozoic, Venkatpur Sandstone Formation, Southern India). *Precambrian Research* **347**, DOI: https://doi.org/10.1016/j.precamres.2020.105854 (2020).

[11] Noffke, N. (ed.) *Geobiology: Microbial Mats in Sandy Depositional Systems from the Archean Era to Today* (Springer, 2010).

[12] Schopf, J. W. Micro-flora of the Bitter Springs Formation, Late Precambrian, central Australia. *Journal of Paleontology* **42**, 651-688 (1968).

[13] Altermann, W. & Nelson, D. R. Sedimentation rates, basin analysis and regional correlations of three Neoarchaean and Palaeoproterozoic sub-basins of the Kaapvaal Craton as inferred from precise U–Pb zircon ages from volcaniclastic sediments. *Sedimentary Geology* **120**, 225-256, DOI: https://doi.org/10.1016/S0037-0738(98)00034-7 (1998).

[14] Schobbenhaus, C. & Kaul, P. F. T. Contribuição à estratigrafia da Chapada Diamantina, Bahia central. Mineração e Metalurgia **53**, 116-120 (1971).

[15] Pedreira da Silva, A. J. C. L. O Supergrupo Espinhaço na Chapada Diamantina Centro-Oriental, Bahia: Sedimentologia, estratigrafia e tectônica. PhD thesis, Universidade de São Paulo, São Paulo (1994).

[16] Souza, E. G. Arquitetura de fácies e evolução estratigráfica dos depósitos eólicos da Formação Mangabeira, Supergrupo Espinhaço - BA. Undergraduate thesis, Universidade Federal do Rio Grande do Sul, Porto Alegre (2012).

[17] Feitosa, A. S. C. Estruturas Sedimentares Induzidas por Microbiais (MISS) na Formação Mangabeira (Mesoproterozoico): Evidências em Depósitos Eólicos e Implicações para a Vida Primitiva. Undergraduate thesis, Universidade Federal de Santa Catarina, Florianópolis (2025).

[18] Bállico, M. B., Scherer, C. M. S., Mountney, N. P., Souza, E. G., Reis, A. D., Raja Gabaglia, G. P. & Magalhães, A. J. C. Sedimentary cycles in a Mesoproterozoic aeolian erg-margin succession: Mangabeira Formation, Espinhaço Supergroup, Brazil. *Sedimentary Geology* **349**, 1-14, DOI: https://doi.org/10.1016/j.sedgeo.2016.12.008 (2017a).

[19] Bállico, M. B., Scherer, C. M. S., Mountney, N. P., Souza, E. G., Chemale, F., Pisarevsky, S. A. & Reis, A. D. Wind-pattern circulation as a palaeogeographic indicator: Case study of the 1.5–1.6 Ga Mangabeira Formation, São Francisco Craton, Northeast Brazil. *Precambrian Research* **298**, 1-15, DOI: https://doi.org/10.1016/j.precamres.2017.05.005 (2017b).

[20] Babinski, M., Pedreira da Silva, A. J. C. L., Brito Neves, B. B. & Van Schmus, W. R. Contribuição à geocronologia da Chapada Diamantina. *In: Anais do VII Simpósio Nacional de Estudos Tectônicos*, 118-120 (Lençóis - BA, 1999).

[21] Silveira, E. M., Söderlund, U., Oliveira, E. P., Ernst, R. E. & Menezes Leal, A. B. First precise U–Pb baddeleyite ages of 1500 Ma mafic dykes from the São Francisco Craton, Brazil, and tectonic implications. *Lithos* **174**, 144-156, DOI: https://doi.org/10.1016/j.lithos.2012.06.004 (2013).

[22] Hunter, R. E. Basic types of stratification in small eolian dunes. *Sedimentology* **24**, 361-387 (1977).
[23] Scherer, C. M. S. & Lavina, E. L. C. Sedimentary cycles and facies architecture of aeolian–fluvial strata of the Upper Jurassic Guará Formation, southern Brazil. *Sedimentology* **52**, 1323-1341, DOI: https://doi.org/10.1111/j.1365-3091.2005.00746.x (2005).
[24] Trewin, N. H. Controls on fluvial deposition in mixed fluvial and aeolian facies within the Tumblagooda Sandstone (Late Silurian) of Western Australia. *Sedimentary Geology* **85**, 387-400 (1993).
[25] Scherer, C. M. S., Lavina, E. L. C., Dias Filho, D. C., Oliveira, F. M., Bongiolo, D. E. & Aguiar, E. S. Stratigraphy and facies architecture of the fluvial-aeolian-lacustrine Sergi Formation (Upper Jurassic), Recôncavo Basin, Brazil. *Sedimentary Geology* **194**, 169-193, DOI: https://doi.org/10.1016/j.sedgeo.2006.06.002 (2007).
[26] Kocurek, G. & Havholm, K. G. Eolian sequence stratigraphy - A conceptual framework. *In*: Posamentier, H. W. & Weimer, P. (eds.) *Siliciclastic Sequence Stratigraphy: Recent Developments and Applications* **58**, 393-409 (AAPG, 1993).
[27] Zhao, C., Shi, M., Feng, Q., Ye, Y., Khan, M. Z. & Feng, F. New study of microbial mats from the Mesoproterozoic Jixian Group, North China: Evidence for photosynthesis and oxygen release. *Precambrian Research* **344**, DOI: https://doi.org/10.1016/j.precamres.2020.105734 (2020).
[28] Noffke, N., Beraldi-Campesi, H., Callefo, F., Carmona, N., Cuadrado, D. G., Hickman-Lewis, K., Homann, M., Mitchell, R., Sheldon, N., Westall, F. & Xiao, S. Microbially Induced Sedimentary Structures (MISS). *In: Treatise Online* (Elsevier, 2022).
[29] Eoff, J. D. Sedimentary facies of the upper Cambrian (Furongian; Jiangshanian and Sunwaptan) Tunnel City Group, Upper Mississippi Valley: New insight on the old stormy debate. *Sedimentary Geology* **302**, 102-121, DOI: http://dx.doi.org/10.1016/j.sedgeo.2013.09.008 (2014).
[30] Riding, R., Fralick, P. & Liang, L. Identification of an Archean marine oxygen oasis. *Precambrian Research* **251**, 232-237, DOI: http://dx.doi.org/10.1016/j.precamres.2014.06.017 (2014).
[31] Azua-Bustos, A., González-Silva, C., Fernández-Martínez, M. Á., Arenas-Fajardo, C., Fonseca, R., Martín-Torres, F. J., Fernández-Sampedro, M., Fairén, A. G. & Zorzano, M.-P. Aeolian transport of viable microbial life across the Atacama Desert, Chile: Implications for Mars. *Scientific Reports* **9**, DOI: https://doi.org/10.1038/s41598-019-47394-z (2019).
[32] Flemming, H. C. & Wingender J. The biofilm matrix. *Nature Reviews Microbiology* **8**, 623-633, DOI: https://doi.org/10.1038/nrmicro2415 (2010).
[33] Decho, A. W. & Gutierrez, T. Microbial Extracellular Polymeric Substances (EPSs) in Ocean Systems. *Frontiers in Microbiology* **8**, DOI: https://doi.org/10.3389/fmicb.2017.00922 (2017).
[34] de Carvalho, C. C. C. R. Biofilms: Microbial Strategies for Surviving UV Exposure. *In*: Ahmad, S. (ed.) *Ultraviolet Light in Human Health, Diseases and Environment, Advances in Experimental Medicine and Biology* **996**, 233-239 (Springer, 2017).
[35] Yin, W., Wang, Y., Liu, L. & He, J. Biofilms: The Microbial "Protective Clothing" in Extreme Environments. *International Journal of Molecular Sciences* **20**, DOI: https://doi.org/10.3390/ijms20143423 (2019).
[36] Belnap, J. & Gillette, D. A. Vulnerability of desert biological soil crusts to wind erosion: the influences of crust development, soil texture, and disturbance. *Journal of Arid Environments* **39**, 133–142, DOI: https://doi.org/10.1006/jare.1998.0388 (1998).[36]
[37] Wältermann, M. & Steinbüchel, A. Neutral Lipid Bodies in Prokaryotes: Recent Insights into Structure, Formation, and Relationship to Eukaryotic Lipid Depots. *Journal of Bacteriology* **187**, 3607-3619, DOI: https://doi.org/10.1128/jb.187.11.3607-3619.2005 (2005).
[38] Finkelstein, D. B., Brassell, S. C. & Pratt, L. M. Microbial biosynthesis of wax esters during desiccation: Adaptation for colonization of the earliest terrestrial environments? *Geology* **38**, 247-250, DOI: https://doi.org/10.1130/G30398.1 (2010).
[39] Langford, R. P. & Chan, M. A. Fluvial-aeolian interactions: Part II, ancient systems. *Sedimentology* **36**, 1037-1051 (1989).
[40] Mountney, N. P. & Thompson, D. B. Stratigraphic evolution and preservation of aeolian dune and damp/wet interdune strata: an example from the Triassic Helsby Sandstone Formation, Cheshire Basin, UK. *Sedimentology* **49**, 805-833, DOI: https://doi.org/10.1046/j.1365-3091.2002.00472.x (2002).
[41] Cain, S. A. & Mountney, N. P. Downstream changes and associated fluvial-eolian interactions in an ancient terminal fluvial system: The Permian Organ Rock Formation, Se Utah, U.S.A. *In*: Davidson, S. K., Leleu, S. & North, C. P. (eds.) *From river to rock record: The preservation of fluvial sediments and their subsequent interpretation* **97**, 167-185 (Society for Sedimentary Geology, 2011).
[42] Chakraborty, T. Sedimentology of a Proterozoic erg: the Venkatpur Sandstone, Pranhita-Godavari Valley, south India. *Sedimentology* **38**, 301-322, DOI: https://doi.org/10.1111/j.1365-3091.1991.tb01262.x (1991).
[43] Belnap, J. & Lange, O. L. Structure and functioning of biological soil crusts: A synthesis. *In*: Belnap, J. & Lange, O. L. (eds.) *Biological Soil Crusts: Structure, Function, and Management*, *Ecological Studies* **150**, 471-479 (Springer, 2001).
[44] Weber, B., Büdel, B. & Belnap, J. (eds.) *Biological Soil Crusts: An Organizing Principle in Drylands* (Springer, 2016).
[45] Noffke, N., Gerdes, G., Klenke, T. & Krumbein, W. E. Microbially Induced Sedimentary Structures - A new category within the classification of primary sedimentary structures. Journal of *Sedimentary Research* **71**, 649-656, DOI: https://doi.org/10.1306/2dc4095d-0e47-11d7-8643000102c1865d (2001).
[46] Harris, B. S., Rozanitis, K. J., Sutherland, B., Myers, P. G., Konhauser, K. O. & Gingras, M. K. Biostabilization: Parameterizing the interactions between microorganisms and siliciclastic marine sediments. *Earth-Science Reviews* **259**, DOI: https://doi.org/10.1016/j.earscirev.2024.104976 (2024).

[47] Gerdes, G. & Klenke, T. Geologische Bedeutung ökologischer Zeiträume in biogener Schichtung (Mikrobenmatten, potentielle Stromatolithe). *Mitteilung der Gesellschaft für Geologie und Bergbaustudien Österreich* **46**, 35-49 (2003).

Acknowledgements

The authors acknowledge the Laboratory of Microscopy and Microanalysis of the Institute of Biological Sciences, University of Brasília (UnB), for providing access to confocal microscopy facilities used in this study. FC acknowledges ANP (grant 2025/21383-2, PRH 43).

Author contributions statement

A.S.C.F. wrote the original draft including the Results, Discussion, and Methods, and prepared the Supplementary Material. M.B.B. conceived the study, participated in fieldwork, wrote the Introduction and Discussion, and revised the manuscript. E.G.S. participated in fieldwork, analysed the results, and contributed to manuscript revision. C.M.S.S. analysed the results and the depositional context, and contributed to manuscript revision. F.C. analysed the results and contributed to the Discussion. A.D.R. participated in fieldwork and assisted in manuscript revision. V.B.A. prepared figures and organized references. G.K.T. prepared figures. E.Y. facilitated access to analytical laboratories. A.M.L. facilitated access to analytical laboratories and assisted in writing the Methods section. S.W.S. conceived the Raman spectroscopy experiments. A.S.S. conceived the Raman spectroscopy experiments. A.M.A.S. conceived the micro-CT experiment and provided partial infrastructure support. R.N.S. conceived the micro-CT experiment.

Additional information

Accession codes: Not applicable; **Competing interests:** The authors declare no competing interests.

Research funding

This research did not receive funding.

Data Availability

The datasets used and/or analysed during the current study are available from the corresponding author on reasonable request.

Supplementary Files

This is a list of supplementary files associated with this preprint. Click to download.

- SupplementaryInformation.docx